IEEE Access
Multidisciplinary | Rapid Review | Open Access Journal

Received November 1, 2017, accepted December 5, 2017, date of publication December 21, 2017, date of current version March 9, 2018.

Digital Object Identifier 10.1109/ACCESS.2017.2785845

Delay and Reliability of Load-Based Listen-Before-Talk in LAA

GORDON J. SUTTON, REN PING LIU, (Senior Member, IEEE), AND Y. JAY GUO, (Fellow, IEEE)

Global Big Data Technologies Centre, University of Technology Sydney, Ultimo NSW 2007, Australia

Corresponding author: Gordon J. Sutton (gordon.sutton@uts.edu.au).

ABSTRACT With the release of the 5 GHz unlicensed spectrum has emerged licensed-assisted access, in which long-term evolution (LTE) operators compete with Wi-Fi users for a share of the unlicensed spectrum so as to augment their licensed spectrum. Subsequently, there has been the need to develop a LTE channel access mechanism that enables harmonious coexistence between Wi-Fi and LTE. Load-based listen-before-talk (LB-LBT) has been adopted as this LTE channel access mechanism by the 3rd Generation Partnership Project (3GPP). Theoretical modelling of LB-LBT schemes has focused on throughput and fair channel-time sharing between Wi-Fi and LTE technologies. We explore a LB-LBT scheme that belongs to LBT category 4, as recommended by the 3GPP, and develop a model for the distribution of the medium access control (MAC) delays experienced by the Wi-Fi packets and LTE frames. The model, validated by simulations, reveals design insights that can be used to dynamically adjust the LB-LBT parameters not only to achieve channel-time fairness, but also to guarantee MAC-delay bounds, with specified probability.

INDEX TERMS MAC delay, licensed-assisted access, load-based equipment, LTE-Wi-Fi coexistence, listen-before-talk, reliability, fairness.

I. INTRODUCTION

Various LBT protocols have been proposed, modelled and/or simulated for LTE/Wi-Fi coexistence [1]–[5]. However, most of the models have concentrated on LTE and Wi-Fi channel-time shares and throughput. Far less attention has been given to MAC delay, with no MAC-delay distribution models offered, to the authors' knowledge. The main aim of this paper is to provide a model for the Wi-Fi packet and LTE-frame MAC-delay distributions when an eNB coexists with Wi-Fi under a LB-LBT channel access protocol.

Some form of assessment of the Wi-Fi traffic by the eNB has been found necessary for LTE to coexist with Wi-Fi in the unlicensed spectrum. Listen-before-talk (LBT), in the LAA context, and channel sensing, in the LTE-U context, both aim to assess the Wi-Fi load. The need for LBT in LAA was demonstrated in [6] and for channel sensing in LTE-U in [7].

3GPP recommended a load-based LBT scheme be employed for LAA in [8]. They defined four LBT categories and recommended the use of Category 4 LBT for downlink LAA. Category 4 LBT schemes are load-based LBT schemes that have a backoff contention window, which introduces an element of random timing to the LTE transmissions that is dependent on the Wi-Fi load.

In the LB-LBT scheme that we model and explore in this paper, a LTE backoff counter is initially selected from a contention window, then decremented each Wi-Fi MAC slot until it reaches zero, at which time the eNB transmits. The approach of synchronising the LB-LBT and Wi-Fi slots is also taken in [2]–[4]. The bounds of the contention window are slowly adapted, based on the Wi-Fi traffic, and the performance is modelled for particular LTE contention window set points, as done in [2] and [3]. The novelty in this paper is that the Wi-Fi packet and LTE-frame MAC delay cumulative distribution functions (CDFs) are modelled.

Wi-Fi MAC-delay CDFs have been obtained by simulation for a small number of LTE/Wi-Fi coexistence settings in [5]. A comparison is made between the eNB transmitting long and short LTE frames, while maintaining a fair channel share. For a given fairness, longer LTE frames lead to longer LTE idle periods and consequently to a higher proportion of Wi-Fi packets being sent without encountering an intervening LTE transmission. This produces short MAC delays for more packets, but also creates substantially longer MAC delays for the packets that encounter an intervening LTE transmission. This principle is demonstrated and quantified by our modelling in this paper.

By developing a model for the Wi-Fi and LTE-frame MAC delays, we can quantify the effects of the Wi-Fi load changing, and of altering the LB-LBT parameters. Parameters considered include the duration of the LTE

frames, the average initial LTE contention window, and the width of the initial LTE backoff window around the average. By monitoring the Wi-Fi traffic, the average initial LTE contention window can be controlled to achieve a particular LTE/Wi-Fi channel time share. The feasibility of achieving a particular LTE throughput, with specified reliability for a specified LTE-frame MAC delay is explored. A feasible region is graphed, given the Wi-Fi traffic and a bound on the LTE channel-time share.

The rest of the paper is organised as follows. A literature review of Wi-Fi MAC-delay modelling is given in Section II. In Section III, our LB-LBT scheme variant is described and justified, and then the system assumptions and components are detailed. In Section IV, an analytical model is developed for the coexistence of our LB-LBT scheme and Wi-Fi, in particular, for the resulting Wi-Fi and LTE-frame MAC-delay distributions. The model is validated in Section V and then used to explore the performance of LB-LBT. Conclusions are given in Section VI.

II. WI-FI MAC-DELAY MODELLING LITERATURE REVIEW

The average MAC delay of the Wi-Fi CSMA/CA DCF protocol, for networks comprising just Wi-Fi stations, i.e., no eNB, has been modelled in different ways. In [9], the average delay for each backoff stage is first calculated from the average times for a collision, successful transmission and a backoff slot. The average MAC delay is then obtained by combining the average delays for each backoff stage. The equation for the average backoff slot duration in [9] is slightly off, which is corrected in [10]. The average total system delay, including both queueing and MAC delay, is modelled in [11] for an unsaturated Wi-Fi network, and the average MAC delay is modelled in [12] for the 802.11 power-save mode when all active Wi-Fi stations simultaneously commence their backoff processes.

A model for the Wi-Fi MAC-delay distribution is introduced in [13] and explored in [14]. The successful transmissions are categorised by the backoff stage in which they succeed and the number of intervening backoff slots from all backoff stages. The MAC-delay distribution for each (backoff stage, number of backoff slots) combination is approximated by a Gaussian distribution, giving the MAC-delay distribution as the weighted sum of the component Gaussian distributions.

The Wi-Fi MAC-delay distribution is also modelled in [15], where the variation in delay is assumed to mainly originate from the random initial backoff counter selection, not the variation in MAC slot durations. The modelled variation is further restricted to that from the initial backoff-counter selection in the backoff stage in which the packet is successful. The resulting expected delays are weighted by their probabilities to approximate the MAC-delay distribution. Despite the simplifications, the MAC-delay distribution model is still quite accurate. Jitter (standard deviation) is also modelled, however this is just a measure of dispersion since the MAC-delay distribution is far from Gaussian.

III. LOAD-BASED LBT AND SYSTEM FRAMEWORK

In this section, the LB-LBT scheme variant explored in this paper is described and justified. The system framework is given first, followed by details of the Wi-Fi and LB-LBT processes.

A. SYSTEM FRAMEWORK

We consider a system comprising N saturated Wi-Fi stations (STAs) and an eNB, operating in an indoor setting with all the nodes within transmission range. Saturated STAs always have a packet ready to transmit, and thus provide the greatest congestion, and a lower limit on the LB-LBT coexists performance. For indoor settings, since the nodes are within close proximity of each other, transmissions are received with high power, so non-colliding transmissions are successfully decoded, whereas colliding transmissions are not, due to the significant interference. The Wi-Fi STAs operate under the 802.11 CSMA/CA protocol, outlined in Section III-B, and the eNB operates under LB-LBT, as described in Section III-C.

Wi-Fi packets comprise a header, containing control information, followed by the data. LTE frames are partitioned in subframes, each starting with control information directing transmissions for the remainder of the subframe, followed by the data [16], [17]. As such, Wi-Fi packets are lost in a collision, whereas only the LTE subframes involved in the collision are lost. Further detail is given when modelling the throughput in Section IV-C.

B. WI-FI CSMA/CA PROCESS

The Wi-Fi STAs follow the CSMA/CA channel-access process. The process is slot-based, with all Wi-Fi STAs making MAC-slot transitions simultaneously. When a packet first reaches head-of-the-line, backoff stage-0 commences with an integer backoff counter selected uniformly from $[0, W_0 - 1]$. At each subsequent MAC slot transition, the counter is decremented, and once it reaches zero, the STA transmits its packet. If the packet collides with another packet, the transmission fails and backoff stage-1 commences, with a new backoff counter selected uniformly from $[0, W_1 - 1]$. The process continues through to a maximum of backoff stage-s, after which a still-unsuccessful packet is dropped. The backoff window doubles in length each backoff stage until backoff stage-m, so that $W_i = W_0 \times 2^{\min(i,m)}$. Further details are omitted because the process is well known and documented.

MAC-slot transitions occur after each slotTime, denoted σ, of channel silence. When a transmission is detected on the channel, the backoff process is deferred until the channel is sensed silent for a continuous DCF interframe space (DIFS), at which time the next MAC-slot transition occurs. The average duration of a Wi-Fi transmission MAC slot is denoted T_{WiFi}.

C. OVERVIEW OF LOAD-BASED LBT PROTOCOL

We consider a LB-LBT mechanism that belongs to the 3GPP's LBT Category 4, as recommended in [8]. The eNB

monitors the channel and uses an energy detection threshold of −62 dBm to sense when the channel is busy.

The general structure of our LB-LBT variant is a slot-based backoff countdown mechanism, with LTE backoff-slot transitions in synchronisation with those for the Wi-Fi CSMA/CA process. That is, the same periods of channel silence, σ and DIFS, are used as for the CSMA/CA protocol to respectively register an unoccupied slot and to resume after the channel is sensed busy.

After each LTE transmission, a new integer initial LTE backoff counter is selected uniformly from $[W_a, W_b]$. The LTE backoff counter is then decremented at each MAC slot transition, and when the counter reaches 0, the eNB transmits. The bounds of the LTE backoff window are slowly adjusted based on monitoring the Wi-Fi traffic, aiming to achieve fair LTE/Wi-Fi channel sharing.

We consider downlink LTE transmissions, sent to multiple user equipment (UE). The LTE frames are taken to have a Type 3 Frame structure so that they can commence anytime, rather than only at licensed-LTE sub-frame boundaries, as adopted by 3GPP [18]. The duration of the LTE transmissions is denoted T_{LTE}. The default T_{LTE} is 10 ms, but the implications of using other T_{LTE} are also considered, as done in [19].

We assume that while monitoring the channel for the LB-LBT procedure, the eNB also maintains an estimate of the probability of each slot being busy and of the average duration of the busy slots. These estimates are then used to adaptively control the LB-LBT contention window. If the LB-LBT contention window is adapted in response to only UE feedback (e.g. HARQ or ACK), then in a congested channel, the LTE contention window could become mostly dependent on the number of Wi-Fi transmissions and largely independent of their durations, thus potentially delivering vastly different LTE and Wi-Fi channel shares for the same number or Wi-Fi users. Some form of channel monitoring to assess the Wi-Fi load by the eNB allows the eNB to choose a target channel-time proportion that achieves fairness and to implement it. The monitoring could be in the form of a Wi-Fi sniffer at the eNB that reads Wi-Fi headers, so as to directly obtain the transmissions times and to estimate the number of active Wi-Fi stations. Since eNBs are mains powered, there would be no significant impediment to them monitoring the channel traffic and reading the Wi-Fi headers as the Wi-Fi stations do. Alternatively, the eNB could maintain an estimate of the probability of a MAC slot being a transmission slot and the average duration of transmission slots, as it monitors the channel for the LB-LBT process.

IV. MAC DELAY MODEL UNDER LB-LBT COEXISTENCE

In this section, models are developed for the cumulative distributions of the Wi-Fi MAC delay and LTE-frame MAC delay. Equations for the LTE channel-time share, and the Wi-Fi and LTE throughput are then given. An equation is then presented for setting the contention window parameters so that the LTE channel-time share is controlled to a target value.

A. WI-FI MAC-DELAY DISTRIBUTION

The MAC slots of a particular saturated Wi-Fi station's (STA's) CSMA/CA process are either backoff slots, in which the STA is deferring, or transmission slots. The transmission slots are in turn either collisions, when another STA or eNB simultaneously transmits, or successes, when the transmission is uncontested. A successful transmission in backoff stage-i, after j backoff slots, occurs after $1+i+j$ MAC slots, comprising j backoff slots, i collision slots and one successful transmission slot. During this process, there may be a number of intervening LTE transmissions.

The Wi-Fi MAC delay is the time from when a Wi-Fi packet starts its backoff process (i.e., becomes head-of-the-line) until just after it is successfully delivered. The cumulative distribution of the Wi-Fi MAC delay is modelled by combining the distribution of the number of MAC slots it takes to successfully deliver a Wi-Fi packet with the distribution of the number of intervening LTE transmissions for each number of MAC slots, and then converting the count distributions to MAC-delay distributions. Expanding on the notation in [13], denote the probability that a Wi-Fi packet is successfully transmitted: in backoff stage-i as $P(i \text{ col})$; after j backoff slots as $P(j \text{ slots})$; and after l LTE transmissions as $P(l \text{ Tx})$. Also, denote the probability that the Wi-Fi MAC delay, d, is less than or equal to D by $P(d \leq D)$. By applying the law of total probability and the chain rule, $P(d \leq D)$ is decomposed as

$$P(d \leq D) = \sum_{i=0}^{s} P(d \leq D | i \text{ col}) P(i \text{ col}) \tag{1}$$

$$= \sum_{i=0}^{s} \sum_{j=0}^{W_i-1} P(d \leq D | j \text{ slots}, i \text{ col}) \times P(j \text{ slots} | i \text{ col}) P(i \text{ col}) \tag{2}$$

$$= \sum_{i=0}^{s} \sum_{j=0}^{W_i-1} \sum_{l=0}^{l_{max}} P(d \leq D | l \text{ Tx}, j \text{ slots}, i \text{ col}) \times P(l \text{ Tx} | j \text{ slots}, i \text{ col}) P(j \text{ slots} | i \text{ col}) \times P(i \text{ col}), \tag{3}$$

where the notation for the conditional probabilities follow from the notation for the marginal probabilities above; and where l_{max} could be as large as $W_i - 1$, but a much lower value is sufficient in practice.

The components of (3) are modelled with constant LTE contention window parameters, as done in [2] and [3], with the intention of using the results to slowly update the LTE contention window. The modelling starts with the distribution of the number of MAC slots taken to successfully transmit a Wi-Fi packet.

1) MAC-SLOT DISTRIBUTION FOR Wi-Fi SUCCESS

The probability $P(j \text{ slots}, i \text{ col})$ is the probability that there are j backoff MAC slots and i collision MAC slots, starting from the MAC slot in which a Wi-Fi packet becomes head-of-the-line (MAC slot 1) through to its successful transmission in

backoff stage-i and MAC slot $j+i+1$. $P(j$ slots, i col) is obtained by modelling the distribution of paths through the Wi-Fi channel-access mechanism for a tagged Wi-Fi STA.

The modelling method is similar to that used in [13]. In [13], the backoff-counter selections for each backoff stage are convolved, to create all the possible paths, and then the conditional MAC-delay distribution for each (j slots, i col) pair is modelled as a Gaussian and the weighted contributions summed. In [13], only Wi-Fi STAs contend for the channel, whereas in the Wi-Fi/LB-LBT coexistence case, there is also an eNB, so an adjustment is made to include the eNB. Since the LB-LBT process introduces relatively long MAC-delay increments, as well as additional modelling complexity, the relatively small-scale conditional MAC-delay distributions around each Wi-Fi (j slots, i col) pair are replaced by the expected value of each (l Tx, j slots, i col) triple.

To model the progress of a tagged STA through the Wi-Fi process, let τ and τ_L be the MAC-slot transmission probabilities for the STAs and eNB respectively, noting that, by symmetry, τ is the same for all STAs. The collision probability observed by the tagged STA, denoted p, is

$$p = 1-(1-\tau)^{N-1}(1-\tau_L), \tag{4}$$

which is solved simultaneously with τ and τ_L. A model for τ is given in [20], which is based on [21], and can be written as

$$\tau = \frac{2(1-p^{s+1})}{(1-p)\sum_{i=0}^{s}(W_i+1)p^i}. \tag{5}$$

The average number of MAC slots per LTE transmission slot is the average initial LTE backoff counter plus one (for backoff count 0), so

$$\tau_L = 1/(1+\frac{W_a+W_b}{2}). \tag{6}$$

$P(j$ slots$|i$ col) is obtained by convolving the probabilities of selecting each initial backoff counter in each backoff stage. Let $w_i[k]$ be the probability of the tagged STA selecting initial backoff counter k in backoff stage-i, $0 \le i \le s$, so that

$$w_i[k] = 1/W_i, \quad 0 \le i \le s,\ 0 \le k < W_i - 1, \tag{7}$$

and

$$P(j \text{ slots}|i \text{ col}) = (w_0 * w_1 * \ldots * w_i)[j]. \tag{8}$$

The probability that the successful transmission by the tagged STA occurs in backoff stage-i, i.e., after i collisions, is

$$P(i \text{ col}) = \frac{(1-p)p^i}{1-p^{s+1}}. \tag{9}$$

2) INTERVENING LTE TRANSMISSION DISTRibution

The probability $P(l$ Tx$|j$ slots, i col) is the distribution of the number of intervening LTE transmissions given a successfully transmitted Wi-Fi packet's path through the backoff process. The distribution depends on the total number of MAC slots, $1+i+j$. The modelling approach taken is to first construct the distribution of the number MAC-slots needed to complete the l^{th} LTE transmission. This distribution is then converted into the distribution of the number of LTE transmissions occurring for a particular number of MAC slots, given there is no LTE transmission in the last MAC slot.

The LTE contention window is parameterised as $[W_a, W_b]$, so the LTE backoff counter can have values 0, .., W_b. After each transmission attempt, a new initial backoff counter is selected from $[W_a, W_b]$. Denote the probability that the LTE backoff counter is k in a random MAC slot by $r[k]$. Then

$$r[k] = \begin{cases} r[k+1], & 0 \le k < W_a, \\ r[k+1] + \dfrac{r[0]}{W_b - W_a + 1}, & W_a \le k \le W_b. \end{cases} \tag{10}$$

Solving (10) gives

$$r[k] \propto W_b + 1 - \max(k, W_a), \quad 0 \le k \le W_b. \tag{11}$$

For saturated Wi-Fi traffic, the first MAC slot of a Wi-Fi packet's backoff process immediately follows a MAC slot in which the eNB could not have transmitted, since the STA's transmission was successful. Let $f[k]$ be the probability that the LTE backoff counter is k in the first MAC slot of a Wi-Fi packet's backoff process, and let $g[k]$ be the probability that the LTE backoff counter is k in the first MAC slot after a LTE transmission. $f[k]$ is approximated as the probability that the LTE backoff counter is k, given the LTE backoff counter did not equal zero in the previous MAC slot. Then,

$$f[k] \propto \begin{cases} r[k+1], & 0 \le k < W_b, \\ 0, & k = W_b, \end{cases} \tag{12}$$

giving

$$f[k] = \frac{W_b - \max(k, W_a - 1)}{(W_b - W_a + 1)(W_b + W_a)/2}, \quad 0 \le k \le W_b, \tag{13}$$

and

$$g[k] = \begin{cases} 0, & 0 \le k < W_a, \\ 1/(W_b - W_a + 1), & W_a \le k \le W_b. \end{cases} \tag{14}$$

Let $B(l,k)$ denote the probability that the l^{th} LTE transmission occurs in the k^{th} MAC slot after a successful Wi-Fi transmission. The probability of there being k LTE backoff slots before the first LTE transmission after a successful Wi-Fi transmission is $f[k]$, and the probability of there being k additional LTE backoff slots before each subsequent LTE transmission is $g[k]$. So, by repeated convolution of $f = [f[0], .., f[W_b]]$ and $g = [g[0], .., g[W_b]]$, and then selecting the index to account for the l LTE transmissions, $B(l,k)$ is obtained as

$$B(l,k) = (f * \overbrace{g * \ldots * g}^{(l-1) \text{ times}})[k-l], \quad l \ge 1,\ k \ge l. \tag{15}$$

Next, let $C(l,k)$ denote the probability that the l^{th} LTE transmission occurs in or before the k^{th} MAC slot after a successful Wi-Fi transmission. $C(l,k)$ is given by the cumulative sum of $B(l,j)$ over j, for a given l, such that

$$C(l,k) = \sum_{j=1}^{k} B(l,j). \tag{16}$$

Then, let $D(l,k)$, $l \geq 0$, $k \geq 1$, be the probability that there are exactly l LTE transmissions from when a Wi-Fi packet becomes head-of-the-line through to the packet's successful transmission, given the successful transmission occurs in the k^{th} MAC slot.

To evaluate $D(l,k)$, consider the different possible paths through the LTE backoff process from the first MAC slot after a successful Wi-Fi transmission. The paths effectively continue on indefinitely, with the successful Wi-Fi transmission MAC slot being a point of observation. $C(l,k-1)$, is the probability that the l^{th} LTE transmission occurs before MAC slot k, so, as the set of paths contributing to $C(l,k-1)$ continue, from after the l^{th} LTE transmission to MAC slot k and beyond, they will similarly include at least l LTE transmissions and have a combined probability mass $C(l,k-1)$.

The paths contributing to $D(l,k)$ require exactly l LTE transmissions before MAC slot k and no LTE transmission in MAC slot k; let $S_D(l,k)$ be the set of paths of length k satisfying these requirements. Also, let $S_C(l,k-1;k)$ be the set of paths contributing to $C(l,k-1)$ and continued to length k, which thus have at least l LTE transmissions before MAC slot k. Then $S_C(l,k-1;k) \supset S_C(l+1,k;k)$ and $S_D(l,k) = S_C(l,k-1;k) \setminus S_C(l+1,k;k)$.

Denote the probability that a path of length k, which might have a LTE transmission at MAC slot k, belongs to $S_D(l,k)$ by $\tilde{D}(l,k)$. Note that $\sum_{l=0}^{\infty} \tilde{D}(l,k) = \sum_{l=0}^{k-1} \tilde{D}(l,k) < 1$, since it excludes all the paths that have a LTE transmission at MAC slot k. So,

$$\tilde{D}(l,k) = \begin{cases} 1 - C(l+1,k), & l = 0, k \geq 1, \\ 0, & l > 0, k = 1, \\ C(l,k-1) - C(l+1,k), & l > 0, k > 1, \end{cases} \tag{17}$$

and

$$D(l,k) = \tilde{D}(l,k) / \left(\sum_{i=0}^{\infty} \tilde{D}(i,k)\right). \tag{18}$$

Then, $P(l \text{ Tx}|j \text{ slots}, i \text{ col})$ is given by

$$P(l \text{ Tx}|j \text{ slots}, i \text{ col}) = D(l, 1+i+j). \tag{19}$$

3) WI-FI MAC DELAY

To evaluate $P(d < D|l \text{ Tx}, j \text{ slots}, i \text{ col})$, the distribution of the MAC delay for each (l,j,i) combination is approximated by its expected value. Let $d(l,j,i)$ be the expected delay for a Wi-Fi packet that is successfully transmitted in the $(1+i+j)^{th}$ MAC slot after it reaches the head-of-the-line, given the packet encountered i collisions and j backoff MAC slots, and there were l LTE transmissions during the process. Then

$$d(l,j,i) = T_{WiFi} + lT_{LTE} + (i+j-l)\frac{iT_{WiFi} + jT_{BO}}{i+j}, \tag{20}$$

where T_{BO} is the expected duration of a backoff slot for the Wi-Fi packet given there is no LTE transmission during the backoff slot, such that

$$T_{BO} = (1-(1-\tau)^{N-1})T_{WiFi} + (1-\tau)^{N-1}\sigma; \tag{21}$$

and

$$P(d \leq D|l \text{ Tx}, j \text{ slots}, i \text{ col}) = \begin{cases} 1, & d(l,j,i) \leq D, \\ 0, & d(l,j,i) > D. \end{cases} \tag{22}$$

The cumulative distribution function (CDF) of the Wi-Fi MAC-delay, $P(d \leq D)$, is then evaluated by combining (3)-(22).

B. LTE-FRAME MAC-DELAY DISTRIBUTION

Define the LTE-frame MAC delay, d_L, as the time from when a LTE frame becomes head of the line until its completed transmission with at least one successful subframe. As mentioned in Section III-C, LAA transmissions can commence anytime [18], and as mentioned in Section III-A, LTE control headers are transmitted at the start of each subframe [16], so in the case of a Wi-Fi/LTE collision, only the subframes involved in the collision are lost. In particular, the first $\lceil T_{WiFi}/T_{sf} \rceil$ subframes will be lost in a collision, where $T_{sf} = 1$ ms is the duration of a subframe and $\lceil \cdot \rceil$ is the ceiling function. With $T_{LTE} > T_{WiFi}$, at least the latter LTE subframes will be successfully transmitted from each LTE frame. Thus, the distribution of d_L will follow the distribution of the LTE backoff process duration, plus T_{LTE}.

Considering a delay budget of D and an initial LTE backoff counter of n, the time for n idle slots, $n\sigma$, and the duration of the LTE frame, T_{LTE}, are sunk costs, whereas each additional Wi-Fi transmission slots costs $T_{WiFi} - \sigma$ on average. As such, given an initial LTE backoff counter of n, a delay budget of D accommodates $\lfloor \frac{D - T_{LTE} - n\sigma}{T_{WiFi} - \sigma} \rfloor$ Wi-Fi transmission slots, where $\lfloor \cdot \rfloor$ is the floor function.

Let P_{Tx} be the probability that at least one Wi-Fi STA transmits in a MAC slot. Then P_{Tx} is given by

$$P_{\text{Tx}} = 1 - (1-\tau)^N, \tag{23}$$

so that, for a given initial number of LTE backoff slots, the number of Wi-Fi transmission slots follows a binomial distribution. The initial LTE backoff counter is distributed uniformly over $[W_a, W_b]$. So, the CDF of the LTE-frame MAC-delay, $P(d_L \leq D)$ is

$$P(d_L \leq D) = \sum_{n=W_a}^{W_b} \frac{F(\frac{D - T_{LTE} - n\sigma}{T_{WiFi} - \sigma}; n, P_{\text{Tx}})}{W_b - W_a + 1}, \tag{24}$$

where $F(k;n,p)$ is the cumulative binomial distribution, which gives the probability of $\lfloor k \rfloor$, or fewer, successes from n trials, each with success probability p, such that

$$F(k;n,p) = \sum_{i=0}^{\lfloor k \rfloor} \binom{n}{i} p^i (1-p)^{n-i}. \tag{25}$$

C. CHANNEL-TIME SHARE AND THROUGHPUT

Denote the average duration of the Idle Period, in which the Wi-Fi STAs have the channel, by $\bar{T}_{Idle}$. Then,

$$\bar{T}_{Idle} = E_s W_{av}, \tag{26}$$

where E_s is the expected duration of a MAC slot given the eNB is not transmitting; and W_{av} is the average number of MAC slots per Idle Period, such that

$$E_s = P_{\rm Tx} T_{WiFi} + (1 - P_{\rm Tx})\sigma, \tag{27}$$

and

$$W_{av} = (W_a + W_b)/2. \tag{28}$$

The LTE channel-time share, denoted ρ_{LTE}, can then be calculated as

$$\rho_{LTE} = \frac{T_{LTE}}{T_{LTE} + \bar{T}_{Idle}}. \tag{29}$$

Denote the average payload per Wi-Fi transmission L_W. Then the Wi-Fi throughput, denoted Thr($WiFi$) is

$$\text{Thr}(WiFi) = \frac{L_W N\tau(1-\tau)^{N-1} W_{av}}{T_{LTE} + \bar{T}_{Idle}}, \tag{30}$$

where $N\tau(1-\tau)^{N-1}$ is the probability of a successful Wi-Fi transmission in a non-LTE-transmission slot.

Each LTE subframe is divided into 14 OFDM symbols. The Control Format Indicator (CFI) specifies the number of OFDM symbols used for control each subframe, with the control signalling occurring in the first CFI symbols of each subframe. As such, the LTE subframes that collide with Wi-Fi transmissions are not decoded and the remaining subframes are decoded. The CFI can equal 1, 2, or 3, depending on the number of UE being supported and needing control information; we use CFI = 2.

Let r_L be the LTE data transmission rate and ϵ_L be the proportion of the LTE-subframe time used to transmit data, so that $\epsilon_L = 1 - \text{CFI}/14$. Then the LTE throughput, denoted Thr(LTE) is

$$\text{Thr}(LTE) = r_L \times \epsilon_L \times \rho_{LTE} \times (1 - \frac{\lceil T_{WiFi}/T_{sf} \rceil}{T_{LTE}/T_{sf}} P_{\rm Tx}), \tag{31}$$

where the last term accounts for subframes lost to Wi-Fi/LTE collisions.

D. SELECTING $[W_a, W_b]$ TO CONTROL ρ_{LTE}

We seek to find a LB-LBT contention window, $[W_a, W_b]$, that achieves a target LTE channel-time share, denoted ρ_{LTE}^{target}, given observed Wi-Fi traffic parameters N and T_{WiFi}, and specified T_{LTE}.

From (4)-(6), (23) and (27), E_S is dependent on W_{av}, but not on W_a or W_b separately. Hence, from (26), $\bar{T}_{Idle}$ also depends on W_{av}, but not on W_a and W_b separately. From (29), ρ_{LTE}^{target}, is achieved for a given T_{LTE} by setting $\bar{T}_{Idle}$ to

$$\bar{T}_{Idle} = \frac{1 - \rho_{LTE}^{target}}{\rho_{LTE}^{target}} T_{LTE}. \tag{32}$$

Equating (32) and (26), the W_{av} that achieves ρ_{LTE}^{target}, denoted W_{av}^{target}, is

$$W_{av}^{target} = \frac{1 - \rho_{LTE}^{target}}{\rho_{LTE}^{target} E_S} T_{LTE}, \tag{33}$$

which can then solved simultaneously with (4)-(6), (23) and (27). A particular window $[W_a, W_b]$ can then be selected so that $W_{av} \approx W_{av}^{target}$. For example, $[W_a, W_b] = [0, 2W_{av}]$ rounded, or $[W_a, W_b] = [0.8W_{av}, 1.2W_{av}]$ rounded.

V. LB-LBT COEXISTENCE PERFORMANCE AND CONTROL

The model developed in Section IV was validated against simulations performed in R [22] for a LAA coexistence scenario comprising an eNB, supporting a number of UE devices, and N Wi-Fi STAs. The eNB and UE were operating under LB-LBT, as presented in Section III-C; and the Wi-Fi STAs were operating under the IEEE 802.11n(20MHz) protocol, as presented in Section III-B. All traffic was simulated as operating in an overlapping coverage area, utilising the same 20 MHz channel within the 5 GHz unlicensed band. The default system parameters are summarized in Table 1, giving $T_{WiFi} = 271$ μs and $T_{LTE} = 10$ ms.

TABLE 1. Simulation settings.

LAA Channel Occupancy Time T_{LTE}			10 ms
LAA Control Format Indicator (CFI)			2 symbol
LAA data rate r_L			100 Mbps
Slot time σ	9 μs	Preamble	36 μs
SIFS	16 μs	Wi-Fi data rate	72.2 Mbps
DIFS	34 μs	Wi-Fi headers	64 byte
W_0	16	Wi-Fi payload L_W	1460 byte
W_m	512	ACK	15.5 μs

A. MODEL VALIDATION

To validate the model, Fig. 1 presents model and simulation Wi-Fi MAC-delay CDFs for a system comprising N saturated Wi-Fi STAs, transmitting 1460-byte packets, resulting in $T_{WiFi} = 271$ μs, and an eNB operating under the LB-LBT protocol described in Section III-C, for a selection of N, T_{LTE} and $[W_a, W_b]$, keeping W_{av} the same. The simulation results were obtained from $N_{frames} = 10^5$ LTE-frame transmissions. The solid-black line and black circles are respectively model and simulation results for ($N = 2$, $T_{LTE} = 2$ ms, $[W_a, W_b] = [0, 100]$); the dashed-red line and triangles are respectively model and simulation results for ($N = 5$, $T_{LTE} = 10$ ms, $[W_a, W_b] = [20, 80]$); and the dotted-blue line and blue pluses are respectively model and simulation results for ($N = 10$, $T_{LTE} = 20$ ms, $[W_a, W_b] = [40, 60]$).

The model and simulation results match closely over the range of settings. The ridges in the CDFs are due to intervening LTE transmissions, with longer T_{LTE} creating longer steps. For higher N, there is more Wi-Fi congestion so that more Wi-Fi packets incur an intervening LTE transmission and the CDF ridges occur at lower probabilities.

Fig. 2 presents the LTE-frame MAC delay CDFs for the same settings as for Fig. 1, using the same legend. Again, the model closely matches the simulation results. The LTE-frame MAC delay is almost linear with the slope dependent on the spread of the LTE contention window, $W_b - W_a$, and N.

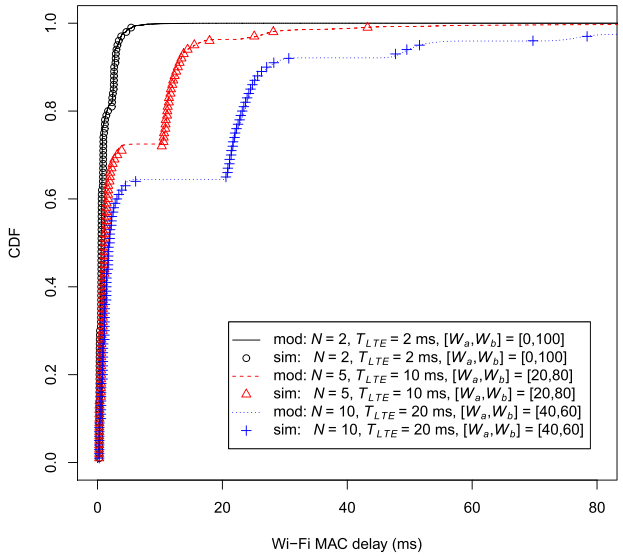

FIGURE 1. Wi-Fi MAC delay CDFs: model validation for selection of N, T_{LTE} and $[W_a, W_b]$; $T_{WiFi} = 271$ μs; $N_{frames} = 10^5$.

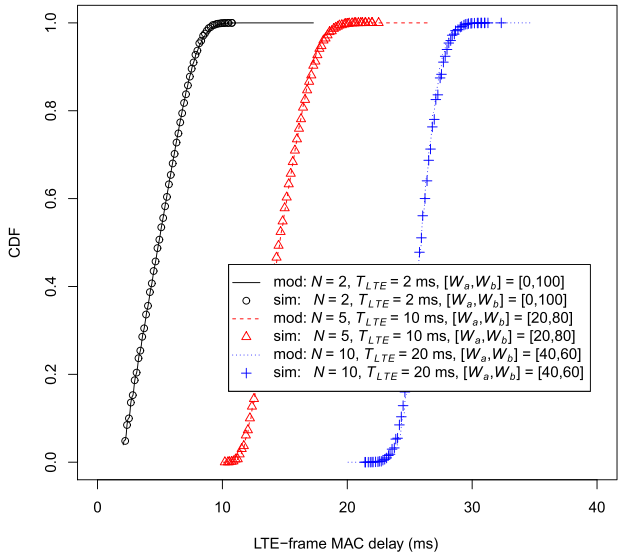

FIGURE 2. LTE-frame MAC delay CDFs: model validation for selection of N, T_{LTE} and $[W_a, W_b]$; $T_{WiFi} = 271$ μs; $N_{frames} = 10^5$.

The effect of T_{LTE} is to offset the whole CDF. When the spread of the LTE contention window, $W_b - W_a$, is narrower, both upper and lower tails are more evident, which is a result of there being fewer component Binomial distributions contributing to the sum in (24).

To further validate the model, 95^{th} percentiles of the Wi-Fi and LTE-frame MAC-delays are presented in Fig. 3 versus N for $T_{LTE} \in \{2, 10, 20\}$ ms and with fixed contention window $[W_a, W_b] = [0, 100]$. The solid-black lines are Wi-Fi model estimates and the dashed-blue lines are LTE model estimates. The circles, triangles and crosses are simulation results for $T_{LTE} = 2$ ms, 10 ms and 20 ms respectively, coloured black for Wi-Fi and blue for LTE, and obtained from $N_{frames} = 10^5$ LTE-frame transmissions.

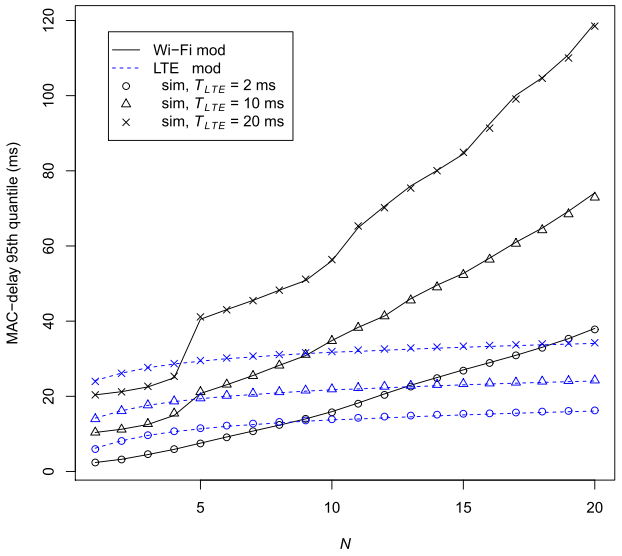

FIGURE 3. MAC-delay 95^{th} percentiles vs. N: $T_{WiFi} = 271$ μs; $T_{LTE} \in \{2, 10, 20\}$ ms; $[W_a, W_b] = [0, 100]$; $N_{frames} = 10^5$.

The model and simulation results match closely in the upper tails of the MAC-delay distributions. The jumps in the Wi-Fi MAC-delay 95^{th} quantiles are due to extra intervening LTE transmissions. With $[W_a, W_b]$ kept constant, the distribution of the numbers of non-transmission, Wi-Fi transmission, and intervening LTE transmission MAC slots contributing to the Wi-Fi MAC delay are independent of T_{LTE}. However, for shorter T_{LTE}, the MAC-delay variation from the Wi-Fi backoff process masks the MAC-delay jumps caused by the LTE transmissions as N increases. The LTE-frame MAC-delay 95^{th} percentiles always include just one T_{LTE}, so they change more smoothly with N and are just offset by changes in T_{LTE}.

B. CHANNEL-TIME SHARE AND THROUGHPUT

Fig. 4 and Fig. 5 present the model LTE throughput Thr(LTE), and model Wi-Fi throughput Thr($WiFi$) respectively, as a function of W_{av}, for $N \in \{1, 2, 5, 10, 20\}$ and $T_{LTE} \in \{2, 10, 50\}$ ms. The LTE contention window shape is set to $[W_a, W_b] = [0, 2W_{av}]$. The black, red and blue lines are for $T_{LTE} = 2$ ms, 10 ms and 50 ms respectively. The value of N is marked on each curve, with solid, dashed, short-dashed, dot-dashed and dotted lines used for $N = 1$, 2, 5, 10 and 20 respectively.

The relationships between the parameters in Fig. 4 are intuitive. Higher N increases the probability of a Wi-Fi transmission MAC slot and thus increases the average LTE backoff slot duration; higher W_{av} directly increases the number of LTE backoff slots; and longer T_{LTE} directly increases the LTE transmission time. As such, ρ_{LTE}, and in turn Thr(LTE), decrease as N increases, decrease as W_{av} is increased, and increase as T_{LTE} is increased.

In contrast, the Thr($WiFi$) curves in Fig. 5 are not monotonic with N, given fixed W_{av} and T_{LTE}. As N increases, Thr($WiFi$) initially increases, since there are more Wi-Fi

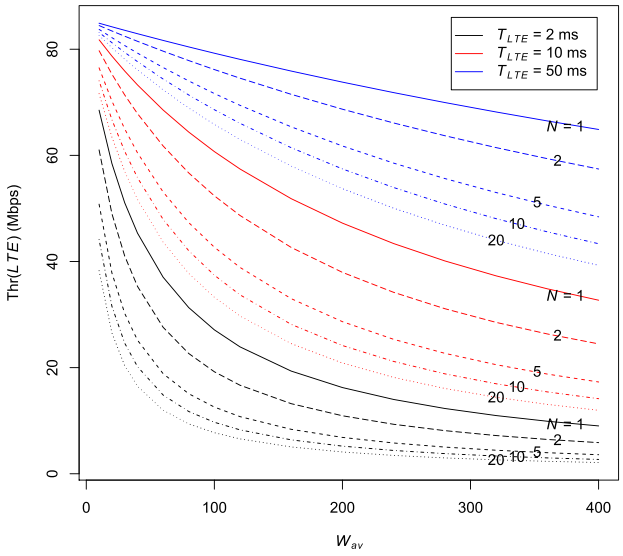

FIGURE 4. LTE throughput Thr(*LTE*) vs. W_{av}: $T_{WiFi} = 271$ μs; $[W_a, W_b] = [0, 2W_{av}]$.

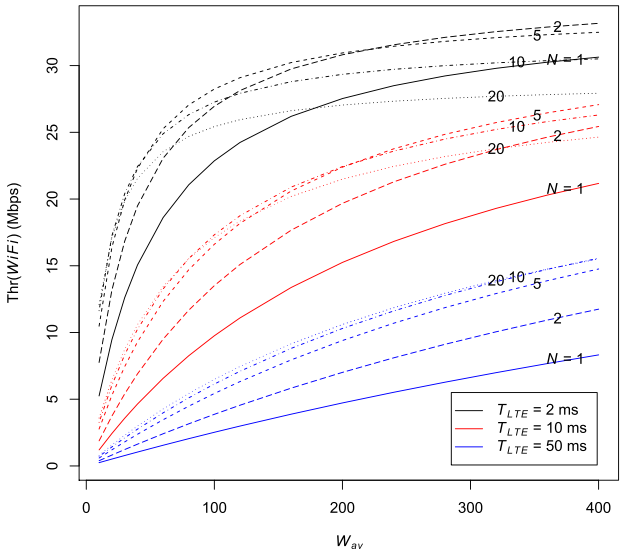

FIGURE 5. Wi-Fi throughput Thr(*WiFi*) vs. W_{av}: $T_{WiFi} = 271$ μs; $[W_a, W_b] = [0, 2W_{av}]$.

transmission attempts during the LTE backoff, on average. As N increases further though, at some value of N, increased Wi-Fi congestion also causes more collisions and reduces Thr(*WiFi*). At this point, increases in N reduce both Thr(*WiFi*) and Thr(*LTE*). The number of STAs needed to cause this throughput-reducing congestion depends both on W_{av} and T_{LTE}.

C. RELIABILITY

For delay-sensitive applications, MAC delay guarantees are more important than throughput guarantees. We define the reliability at MAC delay d as the percentage of transmissions successfully delivered within MAC delay d. Since Wi-Fi/LTE collisions affect the beginnings of LTE frames, transmissions scheduled in the early subframes of a LTE frame, will have lower reliability than those scheduled at the end of the frame. Let the LTE-frame reliability to be the reliability of the latter LTE subframes that do not suffer from Wi-Fi/LTE collisions.

Fig. 6 presents the Wi-Fi reliability at a selection of MAC delays versus N, with $T_{WiFi} = 271$ μs; $T_{LTE} = 10$ ms; and $[W_a, W_b]$ fixed at [0, 100]. The Wi-Fi reliability at MAC delay 100 ms is above 99% for $N < 10$, and drops to 96% between $N = 10$ and $N = 20$. This is indicative of the long MAC-delay distribution tails inherent in the Wi-Fi 802.11 DCF protocol.

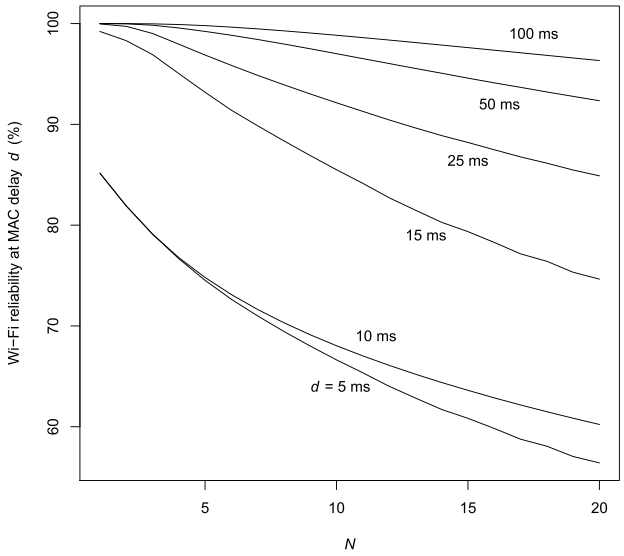

FIGURE 6. Wi-Fi reliability at MAC delay d vs. N: $T_{WiFi} = 271$ μs; $T_{LTE} = 10$ ms; $[W_a, W_b] = [0, 100]$.

Fig. 7 presents the LTE-frame reliability at a different selection of MAC delays versus N, again with $T_{WiFi} = 271$ μs; $T_{LTE} = 10$ ms; and $[W_a, W_b]$ fixed at [0, 100]. The LTE-frame reliability at MAC delay 25 ms is above 99.95% for $N \leq 10$, and, although not shown, the LTE-frame reliability at MAC delay 27.5 ms is above 99.95% for $N \leq 20$, with the same settings.

D. CONTROL

A main requirement of LAA is that LTE shares the unlicensed spectrum fairly with Wi-Fi. We now consider the Wi-Fi and LTE-frame MAC delays when the LTE channel-time share, ρ_{LTE}, is controlled to a particular value.

As mentioned in Section III-C, as a by-product of monitoring the channel for the LB-LBT procedure, we assume the eNB also maintains an estimate of the probability of each MAC slot being busy, P_{Tx}, and of the average duration of the busy slots, T_{WiFi}. A particular ρ_{LTE}^{target} can then be approximately achieved by evaluating E_S from (27), setting W_{av}^{target} according to (33), and setting the LTE backoff window $[W_a, W_b]$ to $[0, 2W_{av}^{target}]$.

The LB-LBT variant being considered allows both W_a and W_b to be changed, and, if the LTE frame structure

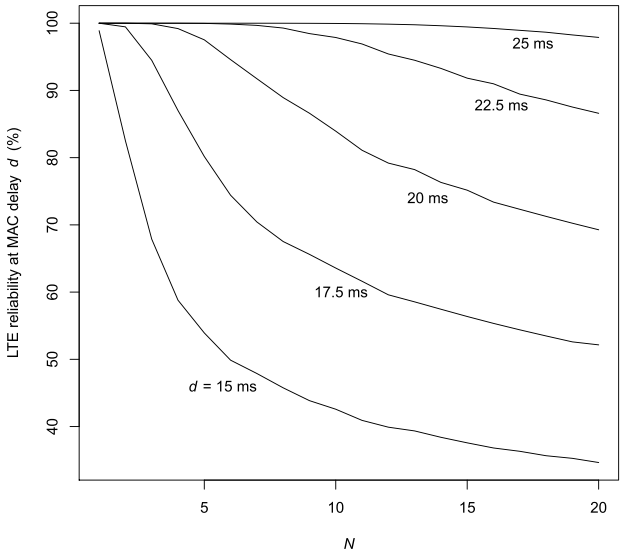

FIGURE 7. LTE reliability at MAC delay d vs. N: $T_{WiFi} = 271$ μs; $T_{LTE} = 10$ ms; $[W_a, W_b] = [0, 100]$.

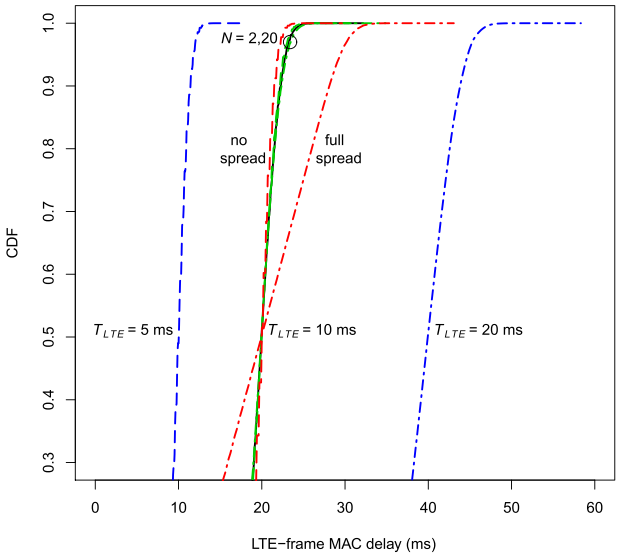

FIGURE 9. LTE-frame MAC-delay CDF showing sensitivity to Wi-Fi load and LB-LBT settings when W_{av} is adjusted to keep $\rho_{LTE} \approx 0.5$. Reference: $N = 10$; $T_{LTE} = 10$ ms; $[W_a, W_b] = [0.8W_{av}, 1.2W_{av}]$; $T_{WiFi} = 271$ μs. Changes: $N \in \{2, 20\}$; $T_{LTE} \in \{5, 20\}$ ms; $[W_a, W_b] \in \{[0, 2W_{av}], [W_{av}, W_{av}]\}$.

permits, T_{LTE} can also be adjusted from the default of 10 ms to other multiples of 1 ms. The sensitivities of the Wi-Fi and LTE-frame MAC delays to these variations, while ρ_{LTE} is maintained at approximately ρ_{LTE}^{target}, are explored in Fig. 8 and Fig. 9.

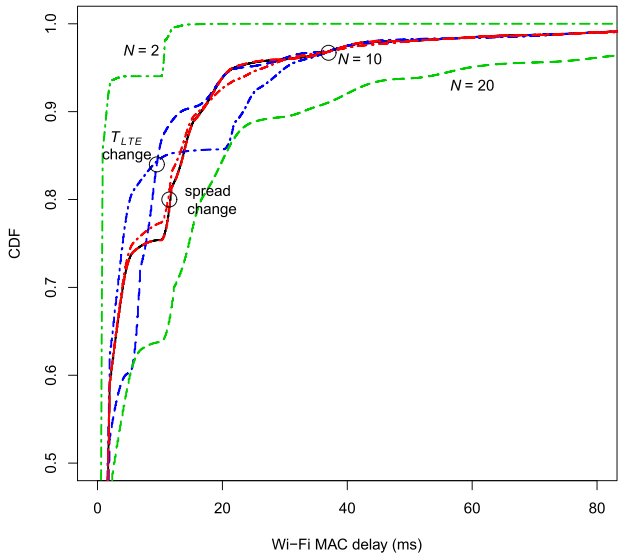

FIGURE 8. Wi-Fi MAC-delay CDF showing sensitivities to Wi-Fi load and LB-LBT settings when W_{av} is adjusted to keep $\rho_{LTE} \approx 0.5$. Reference: $N = 10$; $T_{LTE} = 10$ ms; $[W_a, W_b] = [0.8W_{av}, 1.2W_{av}]$; $T_{WiFi} = 271$ μs. Changes: $N \in \{2, 20\}$; $T_{LTE} \in \{5, 20\}$ ms; $[W_a, W_b] \in \{[0, 2W_{av}], [W_{av}, W_{av}]\}$.

In Fig. 8, Wi-Fi MAC-delay CDFs are presented for a selection of settings around a reference setting. For each setting, W_{av} has been adjusted to keep $\rho_{LTE} \approx 0.5$. The reference setting (solid black line) has $N = 10$, $T_{LTE} = 10$ ms, $T_{WiFi} = 271$ μs, and the LTE backoff window set to $[0.8W_{av}, 1.2W_{av}]$ rounded. To show the sensitivity of the Wi-Fi MAC-delay CDF to Wi-Fi load and LB-LBT parameter changes, N is changed to 2 STAs and 20 STAs (green dot-dashed and dashed lines); T_{LTE} is changed to 5 ms and 20 ms (blue dashed and dot-dashed lines); and the LTE backoff window is set to a full spread, $[0, 2W_{av}]$ rounded, and to no spread, $[W_{av}, W_{av}]$ rounded (red dot-dashed and dashed lines).

As N increases, the Wi-Fi MAC-delay CDF shifts to the right (i.e., the MAC delays become longer); this is as expected since more STAs create more congestion and more intervening Wi-Fi transmissions before a packet is successfully transmitted. As T_{LTE} is increased, the initial ridge in the Wi-Fi MAC-delay CDF shifts higher (i.e., an intervening LTE transmission is less likely) and is longer. However, the CDF tails almost converge by Wi-Fi MAC-delay 40 ms, with cumulated distributions of approximately 97%, regardless of T_{LTE}. As the spread of the LTE backoff window is changed, the change to the Wi-Fi MAC-delay CDF is only slight. So, when ρ_{LTE} is controlled, the Wi-Fi MAC-delay CDF is sensitive to N, but mostly insensitive to both T_{LTE} and LTE backoff-window spread, especially in the upper tail.

Fig. 9 presents LTE-frame MAC-delay CDFs for the same selection of settings as for Fig. 8. The sensitivities are quite different. As N changes, there is almost no change to the LTE-frame MAC-delay CDF. As the LTE backoff-window spread is narrowed from $[0, 2W_{av}]$ to $[W_{av}, W_{av}]$, the LTE-frame MAC-delay CDF also narrows, such that the upper-tail quantiles have shorter MAC delays. As T_{LTE} is increased, the LTE-frame MAC-delay CDF shifts to the right and becomes slightly wider, which is due to the LTE backoff-window spread proportion, $(W_b - W_a)/W_{av}$, being held constant. So, when ρ_{LTE} is controlled, the LTE-frame MAC-delay CDF is insensitive to N, but shorter MAC delays can be

achieved by narrowing the LTE backoff-window spread and by shortening T_{LTE}, if the LTE frame structure permits.

As such, there is the potential to reduce the upper tail of the LTE-frame MAC-delay, and hence increase the LTE-frame reliability at a specified MAC delay, while maintaining a given channel-time proportion, by adjusting the LB-LBT parameters. Narrowing the LTE backoff-window spread comes at little cost and could be set at a particular proportion. If the LTE backoff-window spread is made too narrow though, there is a risk of cyclic collision patterns forming. As a compromise, the LTE backoff-window spread could be set quite narrow, to reduce the LTE-frame MAC delay, while retaining some variation (e.g. $[W_a, W_b] = [0.8W_{av}, 1.2W_{av}]$), which provides some degree of a random walk to the slot-timing of the LTE transmissions. Using a shorter T_{LTE} reduces the LTE-frame delay, but also increases the number of collisions incurred by the earlier LTE subframes, which reduces the LTE throughput. So, there is a trade-off between LTE-frame reliability at a specified MAC delay and LTE throughput. Also, to allow the latter subframes within the LTE frame to be effectively collision free, there will be a practical lower limit on T_{LTE}.

This trade-off is depicted in Fig. 10. Thr(LTE) is plotted against the LTE-frame MAC-delay 99^{th} percentile for different values of ρ_{LTE} and T_{LTE}, with W_{av} evaluated from (33) for each setting. The aim is to assess the possibility of supporting reliable LTE flows on the unlicensed spectrum. As such, only the LTE subframes that contribute to the reliable flows contribute to Thr(LTE). That is, the LTE subframes that commence within T_{WiFi} of the start of each LTE frame are excluded from Thr(LTE), which is then evaluated by setting $P_{\mathrm{Tx}} = 1$ in (31). $[W_a, W_b]$ is set to $[0.8W_{av}, 1.2W_{av}]$; $T_{WiFi} = 271\ \mu$s; and $N = 10$. The solid curves join settings that have the same ρ_{LTE}, and T_{LTE} varies along the curves. The dotted curves join setting that have the same T_{LTE}, and ρ_{LTE} varies along these curves.

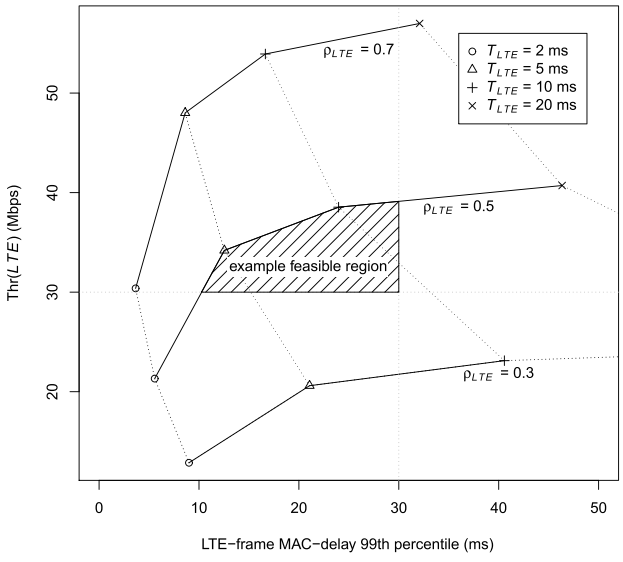

FIGURE 10. Thr(LTE) vs. LTE-frame MAC-delay 99^{th} percentile: $N = 10$; $T_{WiFi} = 271\ \mu$s; W_{av} controlled to give $\rho_{LTE} \in \{0.3, 0.5, 0.7\}$ for indicated T_{LTE}; $[W_a, W_b] = [0.8W_{av}, 1.2W_{av}]$. Example feasible region satisfies constraints: Thr(LTE) $\geq$ 30 Mbps, LTE-frame MAC-delay 99^{th} percentile $\leq$ 30 ms and $\rho_{LTE} \leq 0.5$.

The solid curves show that for a particular ρ_{LTE}, the 99^{th} percentile of the LTE-frame MAC-delay distribution can be reduced, but at the cost of lower Thr(LTE), which is due to an increased proportion of LTE subframes incurring collisions. Fig. 10 can be used to determine whether a LTE (throughput, MAC-delay, channel-time share) combination is feasible. The shaded region, labelled 'example feasible region', satisfies the constraints: Thr(LTE) $\geq$ 30 Mbps, LTE-frame MAC-delay 99^{th} percentile $\leq$ 30 ms and $\rho_{LTE} \leq 0.5$. The bottom-right corner has the lowest ρ_{LTE} and leaves the greatest channel time for Wi-Fi, while satisfying the constraints. The figure is almost independent of N, with slight variation due to quantisation of $[W_a, W_b]$.

VI. CONCLUSION

We developed a model for Wi-Fi and LTE-frame MAC-delay distributions, for an eNB operating under a load-based listen-before-talk (LB-LBT) channel-access scheme and coexisting with Wi-Fi in the unlicensed spectrum. The LB-LBT scheme belongs to LBT Category 4, as recommended by 3GPP, and employs a slot-based backoff process, similar to that used by Wi-Fi stations, with slot transitions synchronised with Wi-Fi MAC slots. The model was validated by simulations, with agreement between the model and simulations in the upper tails of the MAC-delay distributions.

Wi-Fi and LTE throughput and reliability were explored. As expected, the LTE throughput increased with LTE frame duration, decreased with Wi-Fi load and decreased with average initial LTE backoff window length, while Wi-Fi throughput had the opposite interactions. LB-LBT was more reliable than Wi-Fi, with LTE backoff window set to [0, 100]. For example, the LTE-frame reliability was almost 100% at MAC-delay 25 ms, with 20 competing Wi-Fi STAs, whereas the Wi-Fi reliability had dropped to 92% at MAC-delay 25 ms with 10 competing Wi-Fi STAs

The scheme proposed to control the LTE/Wi-Fi channel-time share by adjusting the initial LTE backoff window based on the channel activity, which is monitored while implementing the LB-LBT backoff procedure. With the LTE/Wi-Fi channel-time share maintained at 50%, the upper tail of the Wi-Fi MAC-delay CDF was found to be sensitive to the Wi-Fi load, but insensitive to the LTE parameters. Instead, the LTE-frame MAC-delay CDF was insensitive to the Wi-Fi load, but sensitive to the LTE frame duration and the spread of the initial LTE backoff-window around an average length. In particular, for the same LTE channel-time share, reducing the LTE frame duration and the initial LTE backoff-window spread produces lower LTE delays, while having little impact on the Wi-Fi delay.

The model was used to explore the trade-off between LTE throughput, LTE frame-duration, and LTE-frame MAC delay under LB-LBT for a given channel-time share constraint. An 'example feasible region' was identified that achieved

30 Mbps LTE throughput with 99% reliability at 30 ms LTE-frame MAC-delay, while the process was controlled to meet a 50% channel-share constraint; thereby demonstrating the plausibility of using the unlicensed spectrum for reliable LTE communications.

REFERENCES

[1] C. Chen, R. Ratasuk, and A. Ghosh, "Downlink performance analysis of LTE and WiFi coexistence in unlicensed bands with a simple listen-before-talk scheme," in *Proc. IEEE VTC-Spring*, May 2015, pp. 1–5.

[2] Y. Song, K. W. Sung, and Y. Han, "Coexistence of Wi-Fi and cellular with listen-before-talk in unlicensed spectrum," *IEEE Commun. Lett.*, vol. 20, no. 1, pp. 161–164, Jan. 2016.

[3] F. Hao, C. Yongyu, H. Li, J. Zhang, and W. Quan, "Contention window size adaptation algorithm for LAA-LTE in unlicensed band," in *Proc. Int. Symp. Wireless Commun. Syst. (ISWCS)*, Sep. 2016, pp. 476–480.

[4] Y. Gao, X. Chu, and J. Zhang, "Performance analysis of LAA and WiFi coexistence in unlicensed spectrum based on Markov chain," in *Proc. IEEE Global Commun. Conf. (GLOBECOM)*, Dec. 2016, pp. 1–6.

[5] C. Cano and D. J. Leith, "Unlicensed LTE/WiFi coexistence: Is LBT inherently fairer than CSAT?" in *Proc. IEEE Int. Conf. Commun. (ICC)*, May 2016, pp. 1–6.

[6] R. Ratasuk, N. Mangalvedhe, and A. Ghosh, "LTE in unlicensed spectrum using licensed-assisted access," in *Proc. IEEE Globecom*, Dec. 2014, pp. 746–751.

[7] B. Jia and M. Tao, "A channel sensing based design for LTE in unlicensed bands," in *Proc. IEEE Int. Conf. Commun. Workshop (ICCW)*, Jun. 2015, pp. 2332–2337.

[8] *3rd Generation Partnership Project; Technical Specification Group Radio Access Network; Study Licensed-Assisted Access to Unlicensed Spectrum; (Release 13)*, document 3GPP TR 36.889, V13.0.0, Jul. 2015.

[9] I. N. Vukovic and N. Smavatkul, "Delay analysis of different back-off algorithms in IEEE 802.11," in *Proc. IEEE 60th Veh. Technol. Conf. (VTC-Fall)*, vol. 6. Sep. 2004, pp. 4553–4557.

[10] P. Raptis, V. Vitsas, K. Paparrizos, P. Chatzimisios, A. C. Boucouvalas, and P. Adamidis, "Packet delay modeling of IEEE 802.11 wireless LANs," in *Proc. 2nd Int. Conf. Inf. Technol., Syst. Appl. (CITSA)*, vol. 1, 2005, pp. 71-76.

[11] G. J. Sutton, R. P. Liu, and I. B. Collings, "Modelling IEEE 802.11 DCF heterogeneous networks with Rayleigh fading and capture," *IEEE Trans. Commun.*, vol. 61, no. 8, pp. 3336–3348, Aug. 2013.

[12] R. P. Liu, G. J. Sutton, and I. B. Collings, "WLAN power save with offset listen interval for machine-to-machine communications," *IEEE Trans. Wireless Commun.*, vol. 13, no. 5, pp. 2552–2562, May 2014.

[13] A. Banchs, "Analysis of the distribution of the backoff delay in 802.11 DCF: A step towards end-to-end delay guarantees in WLANs," in *Quality of Service in the Emerging Networking Panorama*. Berlin, Germany: Springer, 2004, pp. 54–63.

[14] A. Banchs, P. Serrano, and A. Azcorra, "End-to-end delay analysis and admission control in 802.11 DCF WLANs," *Comput. Commun.*, vol. 29, no. 7, pp. 842–854, 2006.

[15] P. Raptis, V. Vitsas, and K. Paparrizos, "Packet delay metrics for IEEE 802.11 distributed coordination function," *Mobile Netw. Appl.*, vol. 14, no. 6, pp. 772–781, 2009.

[16] F. Capozzi, G. Piro, L. A. Grieco, G. Boggia, and P. Camarda, "Downlink packet scheduling in LTE cellular networks: Key design issues and a survey," *IEEE Commun. Surveys Tuts.*, vol. 15, no. 2, pp. 678–700, 2nd Quart., 2013.

[17] R. Love *et al.*, "Downlink control channel design for 3GPP LTE," in *Proc. IEEE Wireless Commun. Netw. Conf. (WCNC)*, Las Vegas, NV, USA, Mar./Apr. 2008, pp. 813–818.

[18] *Group Radio Access Network; Evolved Universal Terrestrial Radio Access (E-UTRA); LTE Physical Layer (Release 14)*, document 3GPP TS 36.201 V14.1.0, Mar. 2017.

[19] C. Cano, D. Lopéz-Pérez, H. Claussen, D. J. Leith, "Using LTE in unlicensed bands: Potential benefits and coexistence issues," *IEEE Commun. Mag.*, vol. 54, no. 12, pp. 116–123, Dec. 2016.

[20] H. Wu, Y. Peng, K. Long, S. Cheng, and J. Ma, "Performance of reliable transport protocol over IEEE 802.11 wireless LAN: Analysis and enhancement," in *Proc. IEEE INFOCOM*, vol. 2. Jun. 2002, pp. 599–607.

[21] G. Bianchi, "Performance analysis of the IEEE 802.11 distributed coordination function," *IEEE J. Sel. Areas Commun.*, vol. 18, no. 3, pp. 535–547, Mar. 2000.

[22] *R: A Language and Environment for Statistical Computing. R Foundation for Statistical Computing*, R Core Team, Vienna, Austria, 2015. [Online]. Available: https://www.R-project.org/

GORDON J. SUTTON received the B.Sc. degree in mathematics, the B.E. degree in systems engineering, and the Ph.D. degree in control theory, all from The Australian National University, in 1993, 1995, and 1999, respectively.

He was subsequently with ADC Australia designing optic fibre connectors and then with the Time Series Analysis Section, Australian Bureau of Statistics. In 2006, he joined as a Statistician with the Quantitative Risk Management Stream of CSIRO Mathematics, Informatics and Statistics, Australian CSIRO. In 2011, he joined the School of Chemistry, University of New South Wales, where he was involved in Bayesian statistics and chemometrics. Since 2015, he has been with the Global Big Data Technologies Centre, University of Technology Sydney, involved in modelling Wi-Fi/LTE coexistence protocols. His interests include communications protocol modelling, WLAN, IoT, VANET, LTE, 5G, Markov processes, process analysis and control, forecasting, signal processing, particle filters, state space modelling, and Bayesian statistics.

REN PING LIU (M'09–SM'14) was a Principal Scientist and the Research Leader at CSIRO, where he led wireless networking research activities. He is currently a Professor and the Head of discipline of network and cybersecurity with the School of Electrical and Data Engineering, and the Director of the Cybersecurity Lab, Global Big Data Technologies Centre, University of Technology Sydney. He is also the Research Program Leader of the Digital Agrifood Technologies, Food Agility CRC, a government/research/industry initiative to empower Australia's food industry through digital transformation. He was the Winner of the Australian Engineering Innovation Award and the CSIRO Chairman Medal. He specializes in protocol design and modelling, and has delivered networking solutions to a number of government agencies and industry customers. His research interests include 5G, VANET, IoT, cybersecurity, and blockchain. He has over 100 research publications, and has supervised over 30 Ph.D. students.

Dr. Liu received the B.E. (Hons.) and M.E. degrees from the Beijing University of Posts and Telecommunications, China, and the Ph.D. degree from the University of Newcastle, Australia. He is the Founding Chair of the IEEE NSW VTS Chapter. He served as the technical program committee chair and the organizing committee chair in a number of IEEE Conferences.

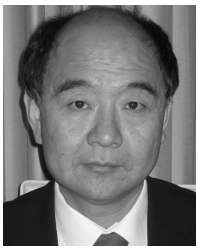

Y. JAY GUO (F'14) received the bachelor's and master's degrees from Xidian University, China, in 1982 and 1984, respectively, and the Ph.D. degree from Xian Jiaotong University, China, in 1987. He held various senior leadership positions in Fujitsu, U.K., Siemens, U.K., and NEC, U.K. He served as the Director of CSIRO for over nine years, directing a number of ICT research portfolios. He is a Distinguished Professor and the Founding Director of the Global Big Data Technologies Centre, University of Technology Sydney, Australia.

He has authored over 350 research papers and holds 22 patents in antennas and wireless systems. His research interest includes antennas, mm-wave and THz communications and sensing systems, and big data. He is a fellow of the Australian Academy of Engineering and Technology and the IET, and a member of the College of Experts of Australian Research Council. He received a number of most prestigious Australian national awards, and was named one of the most influential engineers in Australia in 2014 and 2015.

Dr. Guo has chaired numerous international conferences. He is the International Advisory Committee Chair of the IEEE VTC2017, the General Chair of the ISAP2015, iWAT2014, and WPMC'2014, and the TPC Chair of the 2010 IEEE WCNC, and the 2012 and 2007 IEEE ISCIT. He served as a Guest Editor for special issues on Antennas for Satellite Communications and Antennas and Propagation Aspects of 60–90GHz Wireless Communications, in the IEEE *Transactions on Antennas and Propagation*, Special Issue on Communications Challenges and Dynamics for Unmanned Autonomous Vehicles, the IEEE Journal on Selected Areas in Communications, and Special Issue on 5G for Mission Critical Machine Communications, the *IEEE Network Magazine*.